



# Study on the interaction between a fluorine-containing amphiphilic cationic copolymer and nucleic acid by resonance light scattering technique

Ling Li, Quan Pan, Sheng Dong Xiong, Zu Shun Xu<sup>\*</sup>, Gong Wu Song

Ministry of Education, Key Laboratory for the Synthesis and Application of Organic Function Molecules, Hubei University, Wuhan City, Hubei Province 430062, People's Republic of China

## ARTICLE INFO

### Article history:

Received 30 August 2010  
Received in revised form 31 October 2010  
Accepted 2 November 2010  
Available online 9 November 2010

### Keywords:

Fluorinated cationic amphiphilic graft copolymer  
DNA  
Interaction

## ABSTRACT

A novel fluorine-containing amphiphilic cationic copolymer P(HFMA-St-MOTAC)-g-PEG was synthesized as a new probe to detect DNA based on the RLS technique. The aggregation of P(HFMA-St-MOTAC)-g-PEG on the molecular surface of DNA occurred under pH 4.0–7.0 resulted in an enhanced resonance light-scattering (RLS) peaks at 370 nm, 400 nm, 420 nm and 470 nm. The intensity of resonance light-scattering was found to be proportional to the concentration of DNA. The detection limit was  $5.8 \mu\text{g L}^{-1}$ . It was found that the P(HFMA-St-MOTAC)-g-PEG has strong interaction with DNA as confirmed by the resonance light scattering (RLS) spectroscopy, UV spectra, IR spectra, and TEM.

© 2010 Elsevier B.V. All rights reserved.

## 1. Introduction

The development of novel methods and techniques for determination of DNA is very important in both clinical and laboratory tests. Several kinds of methods have been established to determine the content of DNA in real samples [1–3]. As cationic polymers easily bind to negatively charged phosphate of DNA, this kind of polymers are widely used as one of non-viral vectors because of their interaction with DNA [4,5]. There has been a great deal of the study on the interactions between synthetic cationic polymers and DNA [6,7].

Amphiphilic copolymers consisting of both long hydrophobic and hydrophilic chains have high viscosity and surface activity, and are widely used as gel-formers, surface modifiers, foam and colloid stabilizers, thickeners, wetting agents, compatibilizers, micro-reactors, and nanostructured materials [8]. Poly(ethylene glycol) (PEG) is widely used as the hydrophilic side chain in amphiphilic copolymer. Furthermore, it is an economically and commercially available product possessing useful properties such as solubility both in aqueous and organic solvents, metal complexing ability, biological compatibility, nontoxicity, immunity, biodegradability, and ease of chemical modification [9,10]. Synthesis and application of fluorinated polymers have aroused much interest due to the excellent chemical stability, corrosion resistance, antioxidation, and low surface energy [11].

Although much work has been conducted on the interactions between DNA and amphiphilic copolymers [12–14] or cationic polymers [4,5], detailed characterization of the interactions between DNA and fluorine-containing amphiphilic cationic copolymers is lacked. Fluorine-containing copolymers have been studied from the perspective of biomedical applications, for instance, blood substitutes, gas carriers, bioconversion, extraction, and so forth, which cannot be achieved by non-fluorinated copolymers. Study on the interaction between fluorine-containing copolymers and DNA is expected to open up new applications of fluoro-polymers.

Amphiphilic copolymers containing PEG as the hydrophilic side chains and fluoroalkyl group as hydrophobic side chains are of potential interest because of the unique properties offered by fluoroalkyl unit such as low surface energy, high contact angle, reduced coefficient of friction, biocompatibility, and hydrophobicity [15]. These desirable properties cannot be easily obtained from non-fluorinated amphiphilic graft copolymers [16,17]. In this work, a novel amphiphilic fluorinated copolymer with hydrophobic poly(hexafluorobutyl methacrylate) backbones and poly(ethylene glycol) (PEG) side chains was synthesized and the relationship between the fluorine-containing amphiphilic cationic copolymers and DNA was evaluated.

Since the resonance light scattering (RLS) technique was used to determine DNA concentration in the solution firstly by Pasternack [18,19], has been developed as a sensitive instrumental analysis method.

In this report, resonance light scattering (RLS) technique was adopted as analytical method for the interaction of the prepared

<sup>\*</sup> Corresponding author.

E-mail addresses: [zushunxu@hubu.edu.cn](mailto:zushunxu@hubu.edu.cn), [waitingll@yahoo.com](mailto:waitingll@yahoo.com) (Z.S. Xu).

fluorine-containing amphiphilic cationic copolymer P(HFMA-St-MOTAC)-g-PEG with DNA. It might also be helpful for the development of the application of fluorine-containing amphiphilic cationic copolymers to biomedical purpose.

## 2. Results and discussion

### 2.1. RLS spectral characteristics

Fig. 1 is obtained according to the standard procedure described in experimental Section 4.3. Fig. 1 shows that P(HFMA-St-MOTAC)-g-PEG had four weak RLS peaks at 370 nm, 400 nm, 420 nm, and 470 nm respectively. When ctDNA was added, enhanced RLS peaks could be observed. The phenomena mainly resulted from the aggregation of P(HFMA-St-MOTAC)-g-PEG on the molecular surface of nucleic acid [20]. The extent to which a particle absorbs and scatters light depends on its size, shape, and index of refraction relative to the surrounding medium and scattering. Scattering in each sphere is proportional to the square of the volume.

According to the following formula of RLS [21,22]:

$$I_{\text{RLS}} = \frac{32\pi^3 V^2 n^2 N}{3\lambda_0^4} [(\delta_n)^2 + (\delta_k)^2]$$

where  $n$  is the refractive index of the medium,  $N$  is the molarity of the solution,  $\lambda_0$  is the wavelength of the incident and scattered light,  $V$  is the molecular volume,  $\delta_n$  and  $\delta_k$  are the fluctuations in the real and imaginary components of the refractive index of the particle, respectively. When other factors are constant,  $I_{\text{RLS}}$  is related to the size of the formed particle and directly proportional to the square of molecular volume. Therefore, with the increase of molecular volume of the ion-association,  $I$  is enhanced obviously.

Therefore, the amount of scattering is directly proportional to the volume of each sphere. The larger the aggregation, the greater the scattering. P(HFMA-St-MOTAC)-g-PEG is a cationic amphiphilic graft copolymer, and it is positive ion in solution according to the literature [20,23,24]. As a positively charged molecule, it has a condensing effect on nucleic acids. When the molar ratio of the cationic amphiphilic graft copolymer to nucleic acid is rather high at a lower ionic strength, P(HFMA-St-MOTAC)-g-PEG molecule assembles on the molecular surface of nucleic acid. This leads to long range assembly, which likely induces the formation of

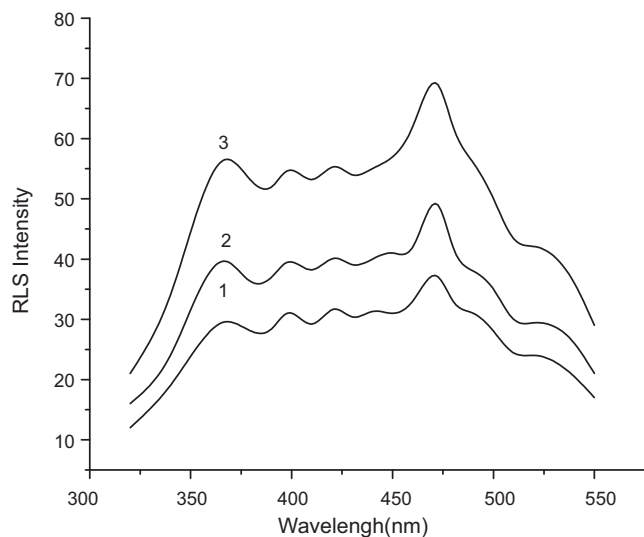


Fig. 1. Resonance light-scanning of P(HFMA-St-MOTAC)-g-PEG/DNA system. P(HFMA-St-MOTAC)-g-PEG: 0.12 mg L<sup>-1</sup>; DNA(1–3): 0 mg L<sup>-1</sup>; 2.4 mg L<sup>-1</sup>; 4.0 mg L<sup>-1</sup>, pH 5.0.

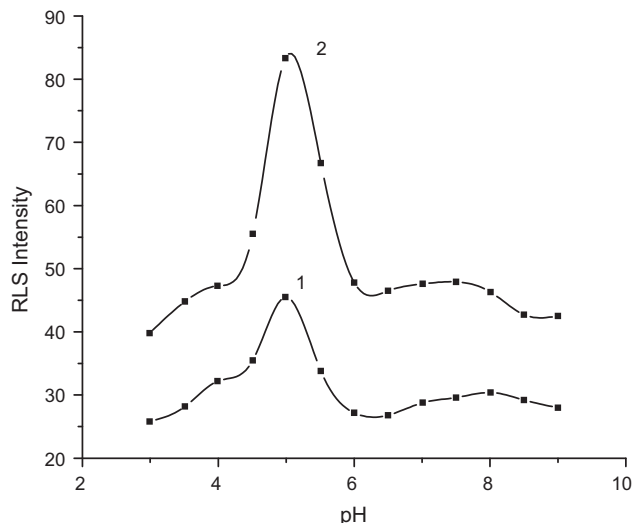


Fig. 2. Effect of pH on the RLS intensity of P(HFMA-St-MOTAC)-g-PEG/DNA system. P(HFMA-St-MOTAC)-g-PEG: 0.12 mg L<sup>-1</sup>; DNA(1–2): 0 mg L<sup>-1</sup>; 2.4 mg L<sup>-1</sup>.

suprahelical structures of nucleic acids. Therefore, since the aggregation of P(HFMA-St-MOTAC)-g-PEG on the molecular surfaces of nucleic acids produces large particles in size, strongly enhanced resonance light scattering can be observed.

### 2.2. Effect of pH

Using Tris-HCl (0.01 mol L<sup>-1</sup>) solution to control the acidity according to the procedure, the intensity of RLS under different acidity was determined. Fig. 2 shows that the RLS intensity of P(HFMA-St-MOTAC)-g-PEG changed little in relation to different acidity. However, the RLS intensity enhanced much when DNA was added. The conformation of DNA changed with acidity of solution, which resulted in the change of RLS intensity. The RLS intensity of P(HFMA-St-MOTAC)-g-PEG/DNA system was weak and not very stable at pH < 3.0 or pH > 9.0, but was stable in the pH range of 4.4–5.5. Therefore, pH 5.0 was selected.

### 2.3. Effect of ionic strength

1.0 mol L<sup>-1</sup> NaCl solution was used to adjust the ionic strength of the system. It could be seen from Fig. 3 that when ionic strength

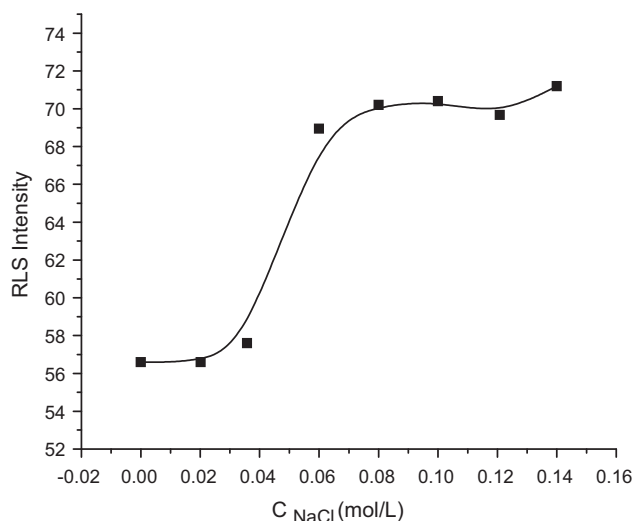


Fig. 3. Effect of NaCl on the RLS intensity of P(HFMA-St-MOTAC)-g-PEG/DNA system. P(HFMA-St-MOTAC)-g-PEG: 0.12 mg L<sup>-1</sup>; DNA: 2.4 mg L<sup>-1</sup>; pH 5.0.

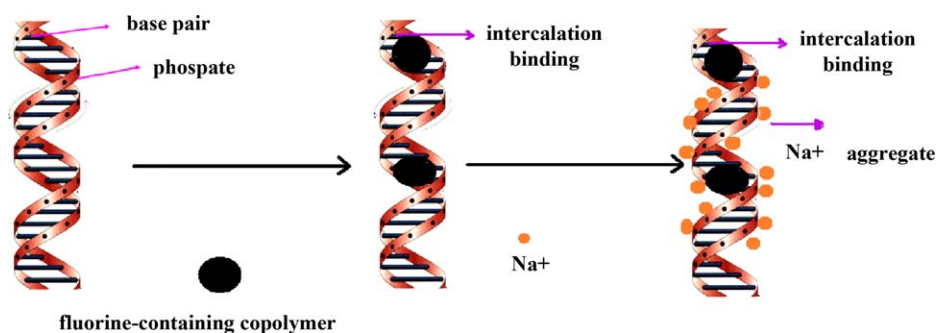


Fig. 4. Effect of  $\text{Na}^+$  on P(HFMA-St-MOTAC)-g-PEG binding to DNA.

was lower than  $0.06 \text{ mol L}^{-1}$ , the system was scarcely affected. Suppose P(HFMA-St-MOTAC)-g-PEG binds to phosphate backbone of DNA by electrostatic binding mode,  $\text{Na}^+$  will aggregate on the negative phosphate backbone of DNA by electrostatic attraction with increasing concentration of NaCl. Therefore, the interaction between P(HFMA-St-MOTAC)-g-PEG and DNA will be affected, and RLS intensity will decrease. If P(HFMA-St-MOTAC)-g-PEG bind to DNA base pairs by intercalation binding mode, the binding will not be affected. Furthermore when  $\text{Na}^+$  continues to assemble on the phosphate backbone of DNA with the increasing NaCl concentration, the particle size will become bigger, so the RLS intensity will increase, as seen in Fig. 4.

P(HFMA-St-MOTAC)-g-PEG is a cationic polymer and it can bind to DNA through electrostatic force. Besides, since it is a fluorinated polymer, which has strong hydrophobic nature, it can bind to DNA through hydrophobic force. The increased RLS intensity proved that the binding mode was intercalation rather than electrostatic interaction, which indicated that hydrophobic force played a major role in the binding.

#### 2.4. Effect of concentration of P(HFMA-St-MOTAC)-g-PEG and calibration curve

The experimental results showed that the enhanced intensity of RLS followed an excellent linear relationship when the concentration of DNA was lower than  $0.5 \text{ mg L}^{-1}$  and the concentration of P(HFMA-St-MOTAC)-g-PEG was in the range of  $3.6 \times 10^{-5}$  to  $7.2 \times 10^{-5} \text{ g L}^{-1}$  for P(HFMA-St-MOTAC)-g-PEG/DNA system. The calibration curve was obtained according to the above standard procedure. There was linear relationship between the RLS intensity and the concentration of DNA. The effect of different concentration of P(HFMA-St-MOTAC)-g-PEG on the linear relationship was displayed in Table 1. It is clear that when the concentration of P(HFMA-St-MOTAC)-g-PEG was in the range of  $4.8 \times 10^{-5}$  to  $7.2 \times 10^{-5} \text{ g L}^{-1}$ , the correlation coefficient of the similar linear regression equation was all excellent and the detection limit was rather low.

#### 2.5. UV-vis spectra

Fig. 5(a) shows that the light absorption of P(HFMA-St-MOTAC)-g-PEG increased at 260 nm when DNA was added, which

can be explained by the interaction between P(HFMA-St-MOTAC)-g-PEG and DNA. Since P(HFMA-St-MOTAC)-g-PEG is polycation in solution, it is easy to attract negatively charged phosphate group of DNA. Fig. 5(b) shows the change of the absorption of DNA at 260 nm when P(HFMA-St-MOTAC)-g-PEG was added. The light absorption of the DNA system increased at 260 nm with the increase in concentrations of P(HFMA-St-MOTAC)-g-PEG, which is also due to the aggregation of P(HFMA-St-MOTAC)-g-PEG on the

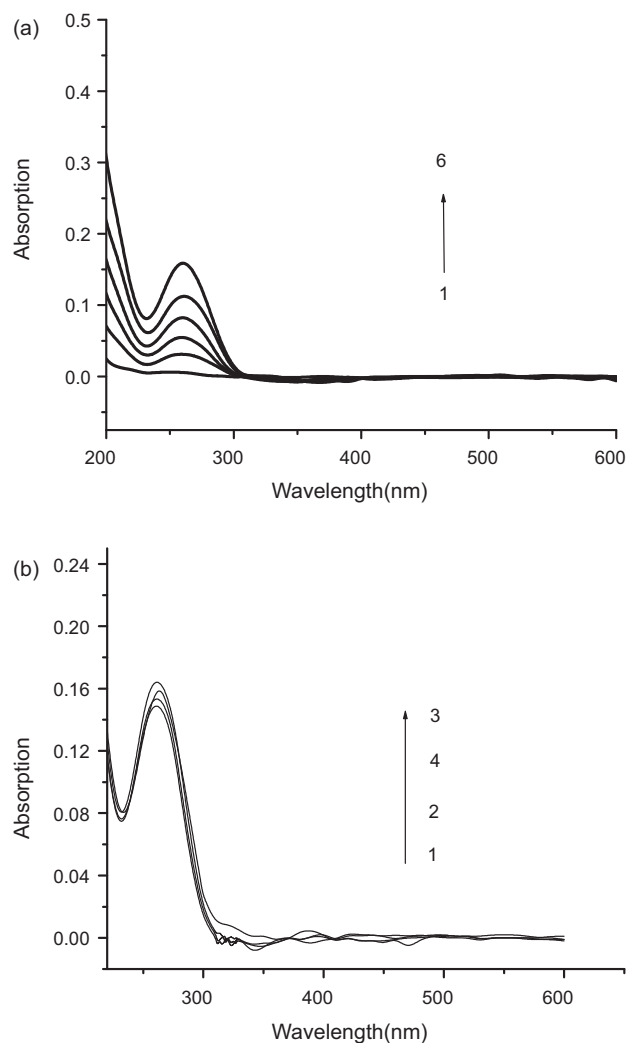


Fig. 5. UV-vis spectra of P(HFMA-St-MOTAC)-g-PEG/DNA complex. (a) P(HFMA-St-MOTAC)-g-PEG:  $0.12 \text{ mg L}^{-1}$ ; DNA(1–5):  $1.8 \text{ mg L}^{-1}$ ,  $3.6 \text{ mg L}^{-1}$ ,  $5.4 \text{ mg L}^{-1}$ ,  $7.2 \text{ mg L}^{-1}$ ,  $9.0 \text{ mg L}^{-1}$ ; (b) DNA:  $9.0 \text{ mg L}^{-1}$ ; (HFMA-St-MOTAC)-g-PEG(1–4):  $0$ ,  $0.048 \text{ mg L}^{-1}$ ,  $0.096 \text{ mg L}^{-1}$ ,  $0.12 \text{ mg L}^{-1}$ .

Table 1  
Effect of concentration of P(HFMA-St-MOTAC)-g-PEG on the linear relationship.

Concentration of P(HFMA-St-MOTAC)-g-PEG ( $\text{g L}^{-1}$ )	Linear regression equation	Correlation coefficient	Detection limit ( $\mu\text{g L}^{-1}$ )
$3.6 \times 10^{-5}$	$I = 41.4C + 22.4$	0.9989	7.5
$4.8 \times 10^{-5}$	$I = 53.3C + 21.1$	0.9989	5.8
$6.0 \times 10^{-5}$	$I = 54.5C + 22.1$	0.9991	5.7
$7.2 \times 10^{-5}$	$I = 53.2C + 23.4$	0.9995	5.8

**Table 2**  
Interference of foreign substances.

No	Foreign substances	Concentration (mg L <sup>-1</sup> )	Change of $\Delta I_{RLS}$ (%)
1	K <sup>+</sup>	1.2	1.6
2	Ba <sup>2+</sup>	5.5	4.2
3	Br <sup>-</sup>	1.0	-2.8
4	Ca <sup>2+</sup>	8.0	-2.4
5	Cu <sup>2+</sup>	2.4	1.7
6	Mn <sup>2+</sup>	22	3.3
7	Al <sup>3+</sup>	0.15	-1.2
8	Ni <sup>2+</sup>	3.2	0.6
9	Zn <sup>2+</sup>	1.2	3.2
10	Fe <sup>3+</sup>	0.6	3.6
11	Cr <sup>3+</sup>	0.8	-4.4
12	RNA	1.6	1.8

molecular surface of nucleic acid. However, by the continuous increase in concentration of DNA, the absorption decreased accompanied by a little red shift from 260 nm to 263 nm. This result can be explained by the intercalation binding between P(HFMA-St-MOTAC)-g-PEG and DNA driven by hydrophobic force. It can be concluded that the binding of P(HFMA-St-MOTAC)-g-PEG to DNA resulted from the experience from aggregation to intercalation with the increase in concentration of P(HFMA-St-MOTAC)-g-PEG [25] (Tables 2 and 3).

## 2.6. IR-spectra

Fig. 6 demonstrates the FT-IR spectra of DNA, P(HFMA-St-MOTAC)-g-PEG, and P(HFMA-St-MOTAC)-g-PEG/DNA complex. The absorbance band at 1656 cm<sup>-1</sup> of DNA shifted to 1648 cm<sup>-1</sup> in P(HFMA-St-MOTAC)-g-PEG/DNA complex would indicate the

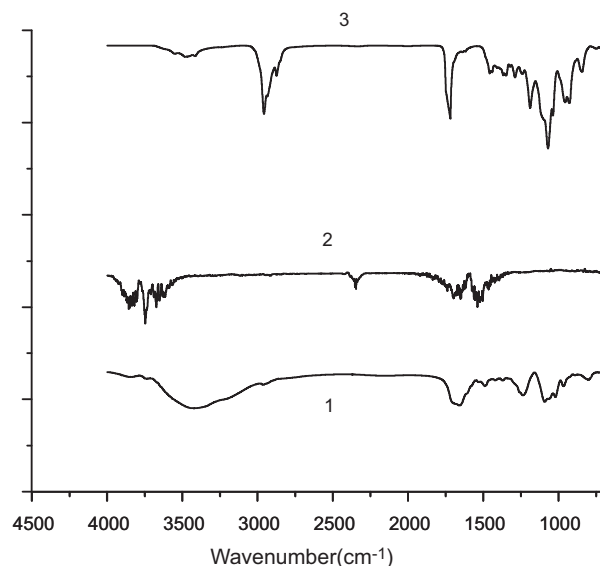


**Fig. 6.** The FT-IR-spectra of P(HFMA-St-MOTAC)-g-PEG/DNA complex. (1) DNA, (2) P(HFMA-St-MOTAC)-g-PEG + DNA, (3) P(HFMA-St-MOTAC)-g-PEG.

interaction between P(HFMA-St-MOTAC)-g-PEG and DNA. The disappearance of the absorption band at 1020, 1093, 1235, 1490 cm<sup>-1</sup> in the P(HFMA-St-MOTAC)-g-PEG/DNA complex would be an evidence for the alteration of the conformation of DNA by the interaction [26].

As for P(HFMA-St-MOTAC)-g-PEG, the characteristic stretching peaks of C=O group are strongly shown at 1700 cm<sup>-1</sup>, resulting from HFMA and MOTAC that contain C=O groups. The absorbance

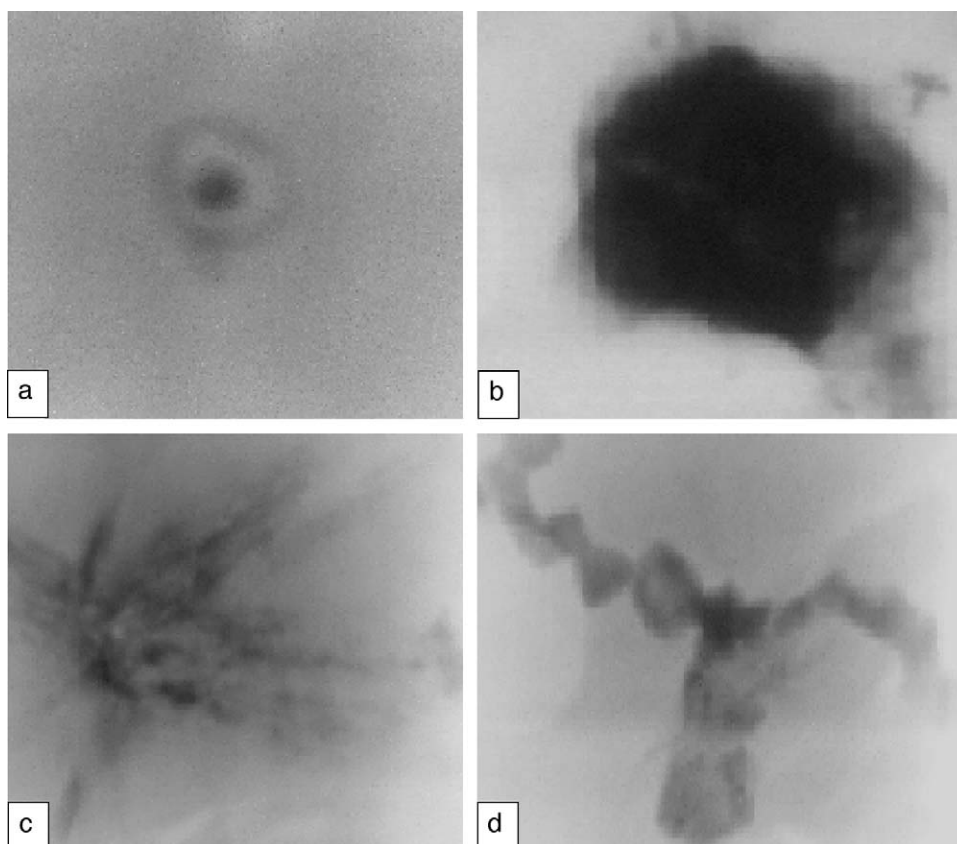


**Fig. 7.** TEM of P(HFMA-St-MOTAC)-g-PEG/DNA complex. (a) 0.048 mg L<sup>-1</sup> P(HFMA-St-MOTAC)-g-PEG; (b) 0.096 mg L<sup>-1</sup> P(HFMA-St-MOTAC)-g-PEG; (c) 0.048 mg L<sup>-1</sup> P(HFMA-St-MOTAC)-g-PEG + 7.2 mg L<sup>-1</sup> DNA; (d) 0.096 mg L<sup>-1</sup> P(HFMA-St-MOTAC)-g-PEG + 7.2 mg L<sup>-1</sup> DNA.

**Table 3**  
Determination result of synthetic samples.

Sample	Concentration of DNA (mg L <sup>-1</sup> )	Foreign substances	Found (mg L <sup>-1</sup> )	Recovery (%)	R.S.D (n=5) (%)
ctDNA	1.6	K <sup>+</sup> , Cu <sup>2+</sup>	1.582	98.9	1.88
ctDNA	1.6	Fe <sup>3+</sup> , Ni <sup>+</sup> , Ca <sup>2+</sup>	1.612	100.8	3.24
ctDNA	1.6	RNA, Zn <sup>2+</sup>	1.626	101.6	1.96

0.2 mg L<sup>-1</sup> K<sup>+</sup>; 0.2 mg L<sup>-1</sup> Cu<sup>2+</sup>; 0.1 mg L<sup>-1</sup> Fe<sup>3+</sup>; 0.5 mg L<sup>-1</sup> Ni<sup>2+</sup>; 0.5 mg L<sup>-1</sup> Ca<sup>2+</sup>; 0.2 mg L<sup>-1</sup> RNA; 0.1 mg L<sup>-1</sup> Zn<sup>2+</sup>; pH 5.0.

at 1453 cm<sup>-1</sup> is the characteristic peak of [-N-(CH<sub>3</sub>)<sub>3</sub>] for MOTAC units. Both the two characteristic absorption peaks disappeared in the P(HFMA-St-MOTAC)-g-PEG/DNA complex, which proved the interaction. The stretching vibration absorption of the C–F bond at 1100–1260 cm<sup>-1</sup> and the stretching vibration absorption of the C–O–C bond at 1250 cm<sup>-1</sup> disappeared in the P(HFMA-St-MOTAC)-g-PEG/DNA complex proving the binding of P(HFMA-St-MOTAC)-g-PEG to DNA.

### 2.7. TEM

Fig. 7(a) and (b) shows that P(HFMA-St-MOTAC)-g-PEG can well self-assemble into spherical micelles in aqueous solution, and the particle size increased (a and b) with the increase in concentration of P(HFMA-St-MOTAC)-g-PEG. The results indicated that self assembly of P(HFMA-St-MOTAC)-g-PEG easily proceeded. Because of the hydrophobic characteristic of the fluorinated segments, during the self-assembly process, they have a high tendency to bury themselves in the interior of the micelles thereby forming the spherical structure.

Morphology features of the aggregates obtained on adding DNA are shown in Fig. 7(c) and (d). From this Fig. 7(a) and (b), the morphology changed significantly, that is, leaf-like for Fig. 7(c) and dendritic structure for Fig. 7(d). When the concentration of P(HFMA-St-MOTAC)-g-PEG was low, DNA bound to P(HFMA-St-MOTAC)-g-PEG molecules weakly, and the main force was electrostatic interaction, then the aggregate formed a leaf-like structure. By the increase in P(HFMA-St-MOTAC)-g-PEG concentration, DNA bound to P(HFMA-St-MOTAC)-g-PEG molecules tightly, and the main force was hydrophobic interaction, then the aggregate formed a dense dendritic structure.

Furthermore, with the enhancement of P(HFMA-St-MOTAC)-g-PEG concentration, the size of sphere increased, and when DNA was added, the size of sphere also increased. These results suggested that hydrophobic interaction plays a major role in binding.

### 3. Conclusion

A novel fluorine-containing amphiphilic cationic copolymer P(HFMA-St-MOTAC)-g-PEG was synthesized and a series of experiments was conducted to investigate and prove the interactions between the P(HFMA-St-MOTAC)-g-PEG and DNA. It was found that P(HFMA-St-MOTAC)-g-PEG had strong interaction with DNA as confirmed by the resonance light scattering (RLS) spectroscopy, UV spectra, IR spectra, and TEM.

The content of HFMA was a main factor affecting the capacity of aggregation [31]. As the rigidity of the C–F bond in P(HFMA-St-

MOTAC)-g-PEG caused stiffening of the hydrophobic chain and interaction with other molecules, its interaction with DNA is strong and it can be used for quantitative determination of DNA. In this study, due to the interaction between P(HFMA-St-MOTAC)-g-PEG and DNA, the large particles are produced resulting in the enhancement of the RLS intensity which is proportional to the concentration of the DNA in a certain range. Based on the linear relationship, the method to determine a trace of DNA was established. Compared to the common fluorimetric method in a spectrofluorimeter, the detection limit is 10 µg L<sup>-1</sup> using ethidium bromide [27] and 0.5 µg L<sup>-1</sup> using ToTo or YoYo [28]. The limit of detection 5.8 µg L<sup>-1</sup> was solved using P(HFMA-St-MOTAC)-g-PEG in this study. It is clear that the technique using P(HFMA-St-MOTAC)-g-PEG is rather sensitive.

In comparison with other substances analyzed by the same light-scattering technique reported, the detection limit was 65.0 µg L<sup>-1</sup> using brilliant green [29] and 10.0 µg L<sup>-1</sup> using mixed complex La(bpy)(phen)Cl<sub>3</sub> [30] respectively. It can be concluded that P(HFMA-St-MOTAC)-g-PEG is applicable to the determination of DNA with high sensitivity.

IR spectra proved that the conformation of DNA was changed by the strong interaction. UV spectra indicated that the interaction between P(HFMA-St-MOTAC)-g-PEG and DNA experienced from aggregation to intercalation with the increase in the concentration of P(HFMA-St-MOTAC)-g-PEG. P(HFMA-St-MOTAC)-g-PEG bound to DNA base pairs by intercalation binding mode mainly induced by hydrophobic force, associated with electrostatic force. TEM photographs proved the binding of P(HFMA-St-MOTAC)-g-PEG to DNA was strong and hydrophobic interaction played a major role in the binding.

### 4. Experimental

#### 4.1. Reagents and chemicals

All reagents were of analytical reagent grade. P(HFMA-St-MOTAC)-g-PEG was synthesized according to the literature [31]. The copolymers were synthesized via conventional free radical polymerization in THF. In a typical reaction, SPEG macromonomer (1.112 g), HFMA (2.800 g), MOTAC (0.088 g), AIBN (0.024 g), and THF (20 mL) were added into a 50 mL round bottom flask equipped with a magnetic stirrer. Then the flask was deoxygenated under reduced pressure and backfilled with nitrogen several times. Polymerization was carried out at 75 °C for 20 h. The product was isolated by evaporating the solvent using a rotary evaporator and then the mixture was precipitated in hexane. After filtration, the precipitate was purified by re-precipitation repeatedly in

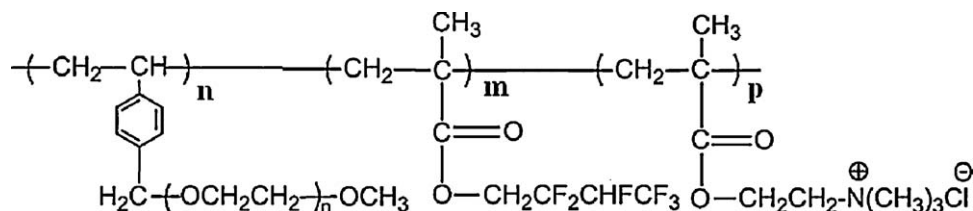


**Fig. 8.** Structure of fluorinated surfactants P(HFMA-St-MOTAC)-g-PEG.

hexane. The obtained product was dried under vacuum at 35 °C for 72 h.

The working solution of P(HFMA-St-MOTAC)-g-PEG was 1.2 mg L<sup>-1</sup>, and the molecular structure of P(HFMA-St-MOTAC)-g-PEG was shown in Fig. 8.

The stock solution of DNA was prepared by dissolving commercially purchased DNA (Sino-American Biotechnology Company, China) in doubly distilled water at 0–4 °C. The working solution of the DNA was 40 mg L<sup>-1</sup>.

0.01 mol L<sup>-1</sup> Tris-HCl solution was used to control the acidity, and 0.1 mol L<sup>-1</sup> NaCl was used to adjust the ionic strength of the aqueous solutions.

Doubly distilled water was used in each experiment.

#### 4.2. Apparatus

The resonance light-scattering spectrum and the intensity of resonance light scattering were measured with a Shimadzu RF-540 spectrofluorometer (Kyoto, Japan). A WH-2 vortex mixer (Huxi Instrumental Co., Shanghai, China) was used to blend the solution, and a PHB-4 pH meter was used to measure the pH value of the solution. The UV-vis spectroscopy and transmittance spectra were acquired from the P(HFMA-St-MOTAC)-g-PEG solutions on the Perkin-Elmer Lambda 17 UV-vis spectrophotometer (USA). The FT-IR spectra of P(HFMA-St-MOTAC)-g-PEG was obtained on Perkin-Elmer Spectrum. While the complex was dried at 25 °C under vacuum, the solid P(HFMA-St-MOTAC)-g-PEG and DNA were used directly to obtain FT-IR spectra. Transmission electron microscopy (TEM) micrographs were obtained by JEM-100SX electron microscope (JEOL, Japan).

#### 4.3. Standard procedure

Appropriate working DNA and P(HFMA-St-MOTAC)-g-PEG solution were added to a 25 mL volumetric flask. The mixture was diluted to 10 mL with doubly distilled water and vortexed. Five minutes later, all the absorption and RLS measurements were obtained against the blank treated in the same way without DNA.

The RLS spectrum was obtained by scanning simultaneously the excitation and emission monochromator of the RF-540 spectrofluorometer through the wavelength range 300–600 nm with  $\Delta\lambda = 0$  nm. The RLS intensity was measured at the maximum wavelength 370 nm.

#### Acknowledgements

The Natural Science Foundation of Hubei Province of China and Ministry-of-Education Key Laboratory for the Synthesis and Application of Organic Functional Molecules supported the work and all the authors here express their deep thanks.

#### References

- [1] L.S. Ling, Z.K. He, G.W. Song, *Anal. Chim. Acta* 403 (2000) 209–217.
- [2] Y.L. Wen, X.Q. Guo, J.G. Xu, *Anal. Chim. Acta* 304 (1997) 291–296.
- [3] C.Z. Huang, Y.F. Li, S.Y. Tong, *Anal. Lett.* 30 (1997) 1305–1319.
- [4] K. Kunath, V.A. Harpe, D. Fischer, H. Peterson, U. Bickel, K. Vougt, *J. Control. Release* 89 (2003) 113–125.
- [5] K. Itaka, K. Yamauchi, A. Harada, K. Nakamura, H. Kawaguchi, K. Kataoka, *Biomaterials* 24 (2003) 4495–4506.
- [6] D.Y. Furgeson, J.W. Yockman, M.M. Janat, S.W. Kim, *Mol. Ther.* 9 (2004) 837–844.
- [7] M. Lee, J. Rentz, M. Bikram, S. Han, D.A. Bull, S.W. Kim, *Gene Ther.* 10 (2003) 1535–1542.
- [8] M.W. Edens, in: V.M. Nace (Ed.), *Nonionic Surfactants: Polyoxyalkylene Block Copolymers*, Marcel Dekker, New York, 1996.
- [9] M. Liu, Z.S. Fu, Q. Wang, J.T. Xu, Z.Q. Fan, *Eur. Polym. J.* 44 (2008) 3239–3245.
- [10] L. Li, S.X. Zheng, *J. Polym. Sci., Part B: Polym. Phys.* 46 (2008) 2296–2306.
- [11] J. Reisinger, M. Hillmyer, *Prog. Polym. Sci.* 27 (2002) 971–976.
- [12] C. Li, X. Liu, L.Z. Meng, *Polymer* 45 (2004) 337–344.
- [13] Y.K. Luu, K. Kim, B.S. Hsiao, B. Chu, M. Hadjiargyrou, *J. Control. Release* 89 (2003) 341–353.
- [14] F.Y. Dai, P.F. Wang, Y. Wang, L. Tang, J.H. Yang, W.G. Liu, H.X. Li, G.C. Wang, *Polymer* 49 (2008) 5322–5328.
- [15] B. Baradie, M.S. Shoichet, *Macromolecules* 38 (2005) 5560–5568.
- [16] H. Hussain, H. Budde, S. Horing, K. Busse, J. Kressler, *Macromol. Chem. Phys.* 203 (2002) 2103–2112.
- [17] H. Hussain, K. Busse, J. Kressler, *Macromol. Chem. Phys.* 204 (2003) 936–946.
- [18] R.F. Pasternack, C. Bustamante, P.J. Collings, A. Giannetto, E.J. Gibbs, *J. Am. Chem. Soc.* 115 (1993) 5393–5399.
- [19] R.F. Pasternack, K.F. Schaefer, P. Hambright, *Inorg. Chem.* 33 (1994) 2062–2065.
- [20] C.Z. Huang, Y.F. Li, N.B. Li, H.Q. Luo, X.H. Huang, *Chin. J. Anal. Chem.* 27 (1999) 1241–1247.
- [21] J. Anglister, I.Z. Steinberg, *J. Chem. Phys.* 78 (1983) 5358–5368.
- [22] J. Anglister, I.Z. Steinberg, *Chem. Phys. Lett.* 65 (1979) 50–54.
- [23] M.J. Carvin, R.J. Fiel, *Nucleic Acids Res.* 11 (1983) 6121–6139.
- [24] C.Z. Huang, K.A. Li, S.Y. Tong, *Anal. Chim. Acta* 345 (1997) 235–242.
- [25] C. Liu, H. Hu, X.M. Chen, *Chin. J. Anal. Lab.* 20 (2001) 30–33.
- [26] Y. He, G.W. Song, Q.C. Zou, Y. He, G.W. Song, Q.C. Zou, *Sens. Actuators B* 106 (2005) 325–331.
- [27] J.B. Le Pecq, C. Paoletti, *Anal. Biochem.* 17 (1996) 100–107.
- [28] H.S. Rye, S. Yue, D.E. Wemmer, M.A. Quesada, R.P. Haugland, R.A. Mathies, A.N. Glazer, *Nucleic Acids Res.* 20 (1992) 2803–2812.
- [29] L. Li, G.W. Song, G.R. Fang, *Am. Biotechnol. Lab.* 25 (2007) 34–35.
- [30] G.W. Song, L. Li, G.R. Fang, *Can. J. Anal. Sci. Spectrosc.* 50 (2005) 60–64.
- [31] S.D. Xiong, L. Li, J. Jiang, L.P. Tong, S.L. Wu, Z.S. Xu, P.K. Chu, *Biomaterials* 31 (2010) 2673–2685.